



Estimating the effect of rainfall on the surface temperature of a tropical lake

Gabriel Gerard Rooney¹, Nicole van Lipzig², and Wim Thiery^{3,4}

¹Met Office, FitzRoy Road, Exeter, EX1 3PB, UK

²KU Leuven, Department of Earth and Environmental Sciences, Celestijnenlaan 200E, 3001 Leuven, Belgium.

³ETH Zurich, Institute for Atmospheric and Climate Science, Universitaetstrasse 16, 8092 Zurich, Switzerland

⁴Vrije Universiteit Brussel, Department of Hydrology and Hydraulic Engineering, Pleinlaan 2, 1050 Brussels, Belgium

Correspondence: G. G. Rooney (gabriel.rooney@metoffice.gov.uk)

Abstract. We make use of a unique high-quality, long-term observational dataset on a tropical lake to assess the effect of rainfall on lake surface temperature. The lake in question is Lake Kivu, one of the African Great Lakes, and was selected for its remarkably uniform climate and availability of multi-year, over-lake meteorological observations. Rain may have a cooling effect on the lake surface by lowering the near-surface air temperature, by the direct rain heat flux into the lake, by mixing the lake surface layer through the flux of kinetic energy, and by convective mixing of the lake surface layer. The potential importance of the rainfall effect is discussed in terms of both heat flux and kinetic-energy flux. To estimate the rainfall effect on the mean diurnal cycle of lake surface temperature, the data are binned into categories of daily rainfall amount. They are further filtered based on comparable values of daily mean net radiation, which reduces the influence of radiative-flux differences. Our results indicate that days with heavy rainfall may experience a reduction in lake surface temperature of approximately 0.3 K by the end of the day compared to days with light-to-moderate rainfall. Overall this study highlights a new potential control on lake surface temperature, and suggests that further efforts are needed to quantify this effect in other regions and to include this process in atmospheric models.

Copyright statement. The works published in this journal are distributed under the Creative Commons Attribution 4.0 License. This licence does not affect the Crown copyright work, which is re-usable under the Open Government Licence (OGL). The Creative Commons Attribution 4.0 License and the OGL are interoperable and do not conflict with, reduce or limit each other.

© Crown copyright 2018

1 Introduction

Lakes are important features of the terrestrial environment for physical, ecological, economic and recreational reasons. Physically, lake-atmosphere interactions can influence the local weather and climate. Thus their representation in earth-system modelling has increased in complexity in recent years. Lake water surface temperature (LWST) is of particular relevance to



atmospheric modelling due to the contrast in temperature, and hence in boundary-layer fluxes, that often exists between lakes and their surroundings (Mironov et al., 2010).

At high latitudes, correct prediction of freezing temperatures, and thus ice-cover periods, is important to obtain accurate boundary-layer fluxes. In the tropics, varying temperature contrasts between lakes and the surrounding land may be associated 5 with cycles of severe weather. For instance, remote sensing data highlight an important impact of the African Great Lakes on the diurnal precipitation and thunderstorm cycle, especially over Lake Victoria and Lake Tanganyika (Camberlin et al., 2017; Thiery et al., 2017). During the afternoon, the typical tropical convective precipitation falls over land, but hardly any rainfall is observed over the lakes. At night, in contrast, very little precipitation is produced over land, while strong convection develops over the lakes, leading to high precipitation amounts. This phenomenon is caused by the diurnal cycle of the lake-land 10 temperature difference, which leads to land breezes converging over the lake surface during the night. When these air masses, moistened by the lake, lift up into the atmosphere, they generate convective precipitation and often thunderstorms (Docquier et al., 2016; Thiery et al., 2015, 2016). The African Great Lakes are thus important regulators of the East African climate, which continues to present a challenge to modellers (James et al., 2018; Woodhams et al., 2018).

Adequately observing and modelling tropical lake-atmosphere interactions often remains a challenge, even though efforts 15 have been made to quantify these exchanges (Verburg and Hecky, 2003; Verburg and Antenucci, 2010; Thiery et al., 2014a, b; Delandmeter et al., 2018; Weyhenmeyer et al., 2017). Moreover, important uncertainties remain present in several of the reference products, notably regarding precipitation (Dinku et al., 2008; Sylla et al., 2013; Awange et al., 2015; Kimani et al., 2017), hence the need for high-quality, in-situ meteorological measurements over the African Great Lakes (Anyah and Semazzi, 2004; Anyah et al., 2006; Anyah and Semazzi, 2009). To help address this need, a state-of-the-art automatic weather station 20 was installed in 2012 on Lake Kivu (AWS Kivu).

Lakes interact with the atmosphere via a variety of processes. Physical lake models developed for use in a meteorological context have thus far concentrated on lake-atmosphere interaction through turbulent and radiative fluxes. The effects of rain on LWST, both directly from thermal perturbation, and indirectly from changing the lake stratification, are little understood or represented to date. Evidence of the significance of rain effects, particularly in the tropics, is beginning to emerge however 25 (Wei et al., 2014). Here, we combine theoretical considerations with analysis of the unique multi-annual dataset from AWS Kivu to estimate the significance of the rainfall effect on LWST in the tropics. As will be shown, the uniformity of the Lake Kivu climate increases its appeal as a location at which to assess this effect.

To summarise the structure of the following sections, in section 2 the study area is described; section 3 discusses the mechanisms of rain effect on LWST; the Kivu data are presented and analysed in section 4; and finally the results are discussed.

30 2 Description of Lake Kivu

The African Great Lakes are of utmost importance for regional economies, as well as being essential to the survival of the local population. As the largest reservoir of freshwater in the tropics, they provide numerous ecosystem services to local communities, such as fishing grounds, drinking water and electricity. Lake Victoria alone directly supports 200 000 fishermen operating



from its shores and sustains the livelihood of more than 30 million people living at its coasts (East African Community, 2011). During the last decades, however, the African Great Lakes experienced fast changes in ecosystem structure and functioning, and their future evolution is a major concern (O'Reilly et al., 2003; Verburg et al., 2003; Verburg and Hecky, 2009; Borges et al., 2015).

5 Lake Kivu ($01^{\circ} 35' S$ - $02^{\circ} 30' S$; $028^{\circ} 50' E$ - $029^{\circ} 23' E$) is situated along the border of Rwanda and the Democratic Republic of Congo, and is one of the seven African Great Lakes (figure 1). The lake has a surface area of 2370 km^2 , lies 1463 m above sea level and is up to 485 m deep. The outflow is located at the lake's southern tip and forms the Ruzizi river, which flows southwards into Lake Tanganyika. Although the lake is meromictic, the oxic mixolimnion deepens to 60-70 m during the dry season. Below that, the monimolimnion is found rich in nutrients and dissolved gases, in particular carbon dioxide and 10 methane (Degens et al., 1973; Borges et al., 2011; Descy et al., 2012; Morana et al., 2015b, a, 2016). Interestingly, temperature and salinity within the monimolimnion increase with depth due to the input of heat and salts from deep geothermal springs (Degens et al., 1973; Spigel and Coulter, 1996; Schmid et al., 2005). Given its high altitude and location close to the equator, surface water temperatures over Lake Kivu are relatively constant throughout the year.

3 Physical effects of rainfall

15 Rain may have an effect on the lake surface in four ways: (i) evaporative cooling of the near-surface air during precipitation, which induces an additional upward sensible heat flux from the lake towards the atmosphere, (ii) by the direct rain heat flux into the lake, (iii) by mixing the lake surface layer through the flux of kinetic energy, and finally (iv) by convective mixing of the lake surface layer. The first of these ought to be parametrised by atmospheric models. The others lie mainly in the lake-modelling domain. Hereafter, we discuss the quantification of these latter effects.

20 3.1 Direct heat flux

The specific heat capacity of water is approximately $4.2 \times 10^3 \text{ J kg}^{-1} \text{ K}^{-1}$. A rainfall rate of 1 mm hr^{-1} is thus equivalent to a heat flux of approximately $1.2 \Delta T \text{ W m}^{-2}$, where ΔT is the temperature difference between the rain and the surface which absorbs it. Rain temperature variation relative to air or surface temperature is not well-known. According to Byers et al. (1949), rain may be much colder than the ambient air at the start of a thunderstorm, but possibly comparable at later stages. This is 25 presumably due to evaporative cooling reducing the air temperature to nearer that of the rain over time, and is consistent with the approximation of the rain temperature to the wet-bulb temperature (Wei et al., 2014, see also references therein).

On seasonal to decadal timescales, the sensible heat contribution by rainfall is deemed small (Verburg et al., 2011). Wei et al. (2014) have estimated that this flux is largest in the tropics, with seasonal mean values of the order of -2 W m^{-2} , and they also state that neglect of this contribution may partly explain some air temperature biases in climate reanalyses. Van Beek 30 et al. (2012) have noted its significance for correctly estimating the surface temperature of tropical rivers. On much shorter timescales, surface cooling due to rain may affect weather patterns.



3.2 Mechanical and convective mixing

As well as the direct effects of an additional heat flux, rainfall may produce a perturbation of LWST by the mechanical and convective mixing of the near-surface portion of the lake. Artificial, heavy rainfall has been shown to produce additional turbulent mixing over depths of 10–20 cm, even in a salt-water body (Lange et al., 2000; Zappa et al., 2009). The entrained air bubbles associated with rainfall are also known to be a significant source of underwater noise energy (Prosperetti et al., 1989).

5 The kinetic energy flux of rainfall has been estimated in the context of soil erosion studies (Salles et al., 2002; van Dijk et al., 2002; Yu et al., 2012). A rain rate of 5 mm h⁻¹ may give rise to a kinetic energy flux F_K of around 0.02 W m⁻², for example. The rate of turbulent kinetic energy (TKE) production in the surface boundary layer of a lake may then be assumed to scale as $F_K/(\rho_w \ell)$ where ℓ is the depth to which the rain penetrates and ρ_w is the water density (see for example Townsend 10 (1976, Ch.2) for a discussion of TKE evolution). The significance of this rain-driven production of TKE may be gauged by comparison with the kinetic energy input from wind shear.

Mechanical surface forcing by wind upon lakes is usually modelled through matching of stress, so that the aqueous friction velocity at the lake surface u_{*l} is

$$u_{*l} = \left(\frac{\rho_a}{\rho_w} \right)^{1/2} u_* \quad (1)$$

15 where u_* is the friction velocity in the atmospheric surface layer, and ρ_a is the air density. A typical atmospheric friction velocity of order 1 m s⁻¹ then implies an aqueous value of $u_{*l} \approx 0.03$ m s⁻¹ (Anctil and Donelan, 1996; Csanady, 2001). The lake surface TKE production from wind-driven shear scales as $u_{*l}^3/(\kappa z)$ where z is the depth and $\kappa = 0.4$ is von Karman's constant (e.g. Skillingstad and Denbo, 1995).

Thus, setting $z = \ell$, the turbulent mixing from rain may be compared to that from wind shear by comparing $u_{*l}^3/(\kappa \ell)$ with 20 $F_K/(\rho_w \ell)$, or equivalently by comparing u_{*l} with $(\kappa F_K / \rho_w)^{1/3}$. This last term is evaluated as of order 0.02 m s⁻¹ for heavy rain, using the value of F_K given above, and is the same order of magnitude as the friction velocity for a moderate-to-strong wind. Hence, the turbulent mixing rates due to wind-shear and rain may at times be comparable in the top few centimetres of a lake.

For cold rain falling onto a relatively warm lake, convective effects will presumably add to the mixing strength and depth. 25 The LWST perturbation caused by mixing effects will depend on the stratification of the lake near-surface region.

4 Data analysis

4.1 Instrumentation and measurements

AWS Kivu is installed on the research platform of the Rwanda Energy Company, approximately 3 km offshore of the cities of Gisenyi (Rwanda) and Goma (D.R. Congo, see figure 2). Since 9 October 2012, AWS Kivu has provided continuous, high-30 quality observations of near-surface meteorology and four-component radiation. The continuous time series obtained so far from AWS Kivu is, to our knowledge, unique of its kind in the tropics.



Table 1. AWS Kivu sensor specifications.

Data	Sensor	Range	Accuracy
Air pressure	Cambell Scientific CS100	600 – 1100 hPa	0.5 hPa
Air temperature	Cambell Scientific CS215	-40 – +70 C	0.3 K
Relative humidity	Cambell Scientific CS215	0 – 100 %	2 – 4 %
Wind speed	Young 05103	0 – 100 m s ⁻¹	0.3 m s ⁻¹
Wind direction	Young 05103	0 – 360°	3°
Precipitation	Tipping Bucket ARG100	0.2 – 500 mm hr ⁻¹	95 – 98 %
SW components	Kipp and Zonen CNR4	305 – 2800 nm	<5 %
LW components	Kipp and Zonen CNR4	4500 – 42000 nm	<10 %

AWS Kivu consists of sensors for air temperature (T_a , C), relative humidity (RH , %), air pressure (p , Pa), precipitation (P , mm), wind speed (U , m s⁻¹) and direction (WD , °) and the four radiation components (SW_{in} , SW_{out} , LW_{in} , LW_{out} , all in W m⁻²). Details of the sensors are given in table 4.1. LWST is calculated from the upwelling longwave irradiance using the Stefan-Boltzmann law and assuming an emissivity of 0.99 (Wan, 2008). The station is powered by a solar panel, and all 5 sensors are placed at a height of 4.40 m above the water surface (a in figure 2), except for wind speed and direction which are measured at 7.20 m above the lake (b in figure 2). Variables are sampled every 15 seconds, from which 30 minute averages are calculated and stored. In the case of precipitation, accumulated values are stored, and for wind speed both mean and maximum values are recorded. Moreover, short periods of high-frequency radiation measurements enable an assessment of the potential 10 effect of platform movements. Through a General Packet Radio Service (GPRS), the KU Leuven Regional Climate Studies group receives the observations directly from the station, allowing for remote problem detection.

The time span of measurements used here was between 13 September 2012 and 14 August 2017, however most of the analysis is based on four calendar years of data from 1 January 2013 to 30 December 2016.

4.2 Weather and climate

The data indicate that there is a remarkable uniformity of the lake climate. The annual air temperature range is around 14 K. 15 The daily rainfall totals for 4 calendar years show a generally uniform spread, but with a slightly drier period around July (figure 3). There seem to be two prevailing wind directions which do not vary greatly with the weather, inasmuch as this is represented by rainfall (see section 4.3). This uniformity is beneficial for the following analysis, since there are consequently fewer sources of variation upon which the lake behaviour may potentially depend.

The temporal variations in weather may be examined further using power spectra of rainfall and wind speed (figure 4). These 20 show that a large part of the variation is on the diurnal scale. This provides justification for the use of average diurnal cycles to explore the behaviour of the system.



4.3 Partitioning by rainfall

To examine the effect of heavy rain, four years of data will be analysed (1 January 2013 to 30 December 2016). This amounts to 1457 days, as three days are omitted due to missing data. These data are referred to as ALL data in the following analysis. Based on daily rainfall totals, they may be divided into DRY, WET and VWET days. DRY days are days with no rainfall. The 5 remaining days are partitioned into WET or VWET depending on whether the rainfall total is respectively less or greater than a threshold of 8 mm (figure 3). The number of days of each type is DRY: 690, WET: 585, VWET: 182.

Regarding the distribution of hourly rainfall over the four years, 2.4% of hours had a rainfall total greater than 1 mm, and 0.6% of hours had a rainfall total greater than 5 mm. Figure 5 shows the average hourly rainfall on WET and VWET days. Both show a minimum in rainfall around 06 UTC (08 LT, LT = UTC + 2 h), and a peak around the middle of the day. There is 10 also a later precipitation maximum in VWET, which may indicate the development of nighttime heavy storms.

The effect of daily weather on LWST is summarised in figure 6. It can be seen that the average diurnal cycles of air temperature and relative humidity are quite smooth, with a spread related to the rainfall category. Thus DRY days are the warmest and least humid, VWET days are the coldest and most humid, and WET and ALL days lie between these extremes. Both the air temperature and LWST start close together for the WET and VWET categories, but by the end of the day there is a difference 15 in the mean, with VWET being colder than WET. Specifically, the average temperature difference over the last 6 hours of the day is 0.42 K.

Atmospheric forcing of LWST is usually characterised in terms of turbulent or radiative fluxes, with turbulent fluxes depending on mean wind speed, lake-air temperature difference and near-surface humidity. For the categories described here, the choice of partitioning threshold between WET and VWET days coincidentally produces extremely similar graphs of mean wind 20 speed. This has the effect of removing an important potential source of variation between these categories. The distributions of wind directions and speeds are also quite uniform, see figures 7 and 8.

Figure 9 shows the difference between the WET and VWET cases in terms of mean net radiation, on average over the course 25 of a day. The lake has absorbed approximately $1.7 \times 10^6 \text{ J m}^{-2}$ more in the WET case. This is due presumably to WET days having less (or less thick) cloud cover than VWET days on average. This source of difference may be eliminated by adding a further constraint to the total absorbed radiation on WET days. This is described in the next subsection.

4.4 Further partitioning by rainfall and net radiation

WET days have a higher mean net radiation than VWET days (figure 9). To separate the effects of rainfall and radiation, the WET days may be further filtered for those with integrated net radiation below a specified amount, so that the mean value is reduced to equal to, or less than, that on VWET days. This subset of “dull” WET days is labelled DWET. With a threshold 30 total radiation of $1.5 \times 10^7 \text{ J m}^{-2}$, the average total radiation of DWET days is approximately $1.03 \times 10^7 \text{ J m}^{-2}$, compared to an average total radiation of $1.05 \times 10^7 \text{ J m}^{-2}$ on VWET days. Using this additional constraint, the number of DWET days in the 4-year period is 425, or 73% of the WET days. The distributions of wind directions and speeds for the DWET category



are also plotted in figures 7 and 8. The diurnal cycle of the mean net radiation difference between DWET and VWET cases is shown in figure 9.

The average daily rainfall on DWET days is 2.31 mm, compared to 2.33 mm on WET days and 17.99 mm on VWET days. Thus, the contrast in rainfall amount is largely preserved by this resampling. The diurnal evolution is also plotted in figure 5, 5 again showing that DWET is similar to WET.

The average diurnal evolution for the categories of ALL, DRY, DWET and VWET is shown in figure 10. It can be seen that the evolution of diurnal wind speed is reasonably unchanged for DWET days compared to that of WET days (figure 6), but the evolution of LWST on DWET days is closer to that of VWET days. However, most of the difference in surface temperature between these categories in the last few hours of the day remains, with an average temperature difference over the last 6 hours 10 of 0.29 K.

Considering the reliability of this difference, it may be noted that a difference of 0.3 K against a background at approximately 300 K is equivalent to a difference in upwelling longwave of approximately 1.8 W m^{-2} . However, since this is a difference between mean values taken over a minimum of 182 observations at each time of day, it should be compared with the standard error of the mean. That is, it only requires instrumental accuracy of $1.8 \times \sqrt{182} \approx 24 \text{ W m}^{-2}$, which is within the instrument 15 specification (table 4.1).

In terms of significance, the standard error of the difference between the mean DWET and VWET values is given by

$$SED = \sqrt{\frac{\sigma_{DWET}^2}{N_{DWET}} + \frac{\sigma_{VWET}^2}{N_{VWET}}} \quad (2)$$

where σ_{DWET}^2 and σ_{VWET}^2 are the variances of LWST in the DWET and VWET cases respectively, and the number of observations at any particular time of day are $N_{DWET} = 425$ and $N_{VWET} = 182$, as stated earlier. SED takes values in the range 0.05–0.07 K 20 during the first and last few hours of the day, climbing to over 0.14 K during daylight hours. The hypothesis that the means are equal may be tested using the difference in mean values divided by SED (e.g. Frank and Althoen, 1994, chapter 10). This is plotted in figure 11. It can be seen that, before 16 UTC, this statistic takes values in the approximate range $[-2, 2]$, indicating that the hypothesis of equal means may be accepted at approximately the 5% level of significance at these times. However, after 17 UTC, this statistic climbs to values well above 2, indicating that the hypothesis may reasonably be rejected at later 25 times. It is therefore concluded that the difference in the means during the last few hours of the day is statistically significant.

5 Discussion and Conclusion

Lake Kivu has a remarkably stable tropical lake climate, and AWS Kivu has yielded a high-quality, multi-year, over-lake observational record which is rare and perhaps unique in the tropics, and well-suited to the present research question. This study is the first such use of these data.

30 Data over four years from AWS Kivu have been categorised by daily rainfall amount and net radiation, to investigate the possible effects of rainfall on lake water surface temperature (LWST), which may be particularly significant in the tropics (Wei et al., 2014). The choice of division between days with heavy or light-to-moderate rain (respectively greater or less than 8 mm



total) has helped minimise the sources of difference between the categories other than that due to rainfall. Spectral analyses have shown that, in this uniform climate, one of the dominant variations is the diurnal cycle, and hence the different categories are compared via their mean diurnal evolution. In the mean data examined here, heavy rain on a tropical lake would seem to have the capability to produce a reduction of a few tenths of one Kelvin in LWST over the course of several hours at the end of 5 the day, compared to light-to-moderate rain; and this reduction is statistically significant.

The possible pathways by which this effect may arise are: (i) cooling of the air due to contact with evaporatively-cooled raindrops, and a subsequent increase in atmospheric sensible heat flux from the lake, (ii) negative heat flux directly to the lake from rain impingement, (iii) mechanical mixing of the lake surface layer by the kinetic energy of rain impact, and (iv) convective mixing of the lake surface layer due to the negative heat flux from rain. Of these, the first is the most likely to be 10 a parametrised process in a General Circulation Model of the atmosphere, although it could be considered the most indirect of the four. The rain heat flux is likely to be proportional to the difference between the air wet-bulb temperature and LWST. We have indicated with scaling arguments that the mechanical mixing due to heavy rain may be comparable to that of a strong wind. The convective mixing will depend on the near-surface temperature structure of the lake, and hence on its recent history.

Unfortunately, the available data do not cover several other process-related quantities that would be useful to have, such 15 as turbulent heat fluxes, rain temperature, fine-scale lake temperature profiles or lake turbulence measurements. Thus, the processes producing this effect are not directly measured. However, through our indirect analysis of the processes it seems likely that cooling by rain combined with mechanical and convective mixing from droplet impact may have an effect on LWST.

In large tropical lakes, it is possible that a surface temperature difference of order half a Kelvin may suppress or enhance the 20 strength of local air circulations, such as lake breezes, and hence have some effect (or even feedback) on the evolution of the local weather (Thiery et al., 2015, 2016). For example, the length of time between severe storms may be partly affected by the recovery timescale of LWST. It would seem possible to incorporate, perhaps semi-empirically, the effect of rain temperature and rain-induced turbulence into simple lake models as used for weather and climate modelling. Potential avenues of future work would be to examine these processes more closely in a targeted campaign of observations, including the quantities listed 25 above, and to consider how lake models may be modified to include their representation.

Acknowledgements. WT was supported by an ETH Zurich postdoctoral fellowship (Fel-45 15-1). The Uniscentia Foundation and the ETH Zurich Foundation are thanked for their support to this research. The Belgian Science Policy Office (BELSPO) is acknowledged for the support through the research project EAGLES (CD/AR/02A). We thank Stijn Bruggen, who analysed the AWS data in his Master's thesis, and thereby supported the design of this study and the analysis presented here. GGR thanks John M. Edwards for a helpful discussion of 30 TKE budgets.



References

F. Anctil and M. Donelan. Air–water momentum flux observations over shoaling waves. *Journal of Physical Oceanography*, 26(7):1344–1353, 1996.

R. O. Anyah and F. Semazzi. Idealized simulation of hydrodynamic characteristics of Lake Victoria that potentially modulate regional climate. *International Journal of Climatology*, 29:971–981, 2009.

R. O. Anyah and F. H. M. Semazzi. Simulation of the sensitivity of Lake Victoria basin climate to lake surface temperatures. *Theoretical and Applied Climatology*, 79(1-2):55–69, 2004.

R. O. Anyah, F. H. M. Semazzi, and L. Xie. Simulated Physical Mechanisms Associated with Climate Variability over Lake Victoria Basin in East Africa. *Monthly Weather Review*, 134:3588–3609, 2006.

J. Awange, V. Ferreira, E. Forootan, Khandu, S. Andam-Akorful, N. Agutu, and X. He. Uncertainties in remotely sensed precipitation data over Africa. *International Journal of Climatology*, 2015.

A. V. Borges, G. Abril, B. Delille, J.-P. Descy, and F. Darchambeau. Diffusive methane emissions to the atmosphere from Lake Kivu (Eastern Africa). *Journal of Geophysical Research*, 116:G03032, 2011.

A. V. Borges, F. Darchambeau, C. R. Teodoru, T. R. Marwick, F. Tamooh, N. Geeraert, F. O. Omengo, F. Guérin, T. Lambert, C. Morana, E. Okuku, and S. Bouillon. Globally significant greenhouse-gas emissions from African inland waters. *Nature Geoscience*, 8, 2015.

H. R. Byers, H. Moses, and P. J. Harney. Measurement of rain temperature. *J. Met.*, 6:51–55, 1949.

P. Camberlin, W. Gitau, O. Planchon, V. Dubreuil, B. M. Funatsu, and N. Philippon. Major role of water bodies on diurnal precipitation regimes in Eastern Africa. *International Journal of Climatology*, 2017.

G. T. Csanady. *Air-sea interaction: laws and mechanisms*. Cambridge University Press, 2001.

E. Degens, R. Von Herzen, H.-K. Wong, W. Deuser, and H. Jannash. Lake Kivu: Structure, chemistry and biology of an East African rift lake. *Geologische Rundschau*, 62:245–277, 1973.

P. Delandmeter, J. Lambrechts, V. Legat, V. Vallaeys, J. Naithani, W. Thiery, J.-F. Remacle, and E. Deleersnijder. A fully consistent and conservative vertically adaptive coordinate system for SLIM 3D v0.4 with an application to the thermocline oscillations of Lake Tanganyika. *Geoscientific Model Development*, 11(3):1161–1179, 2018.

J.-P. Descy, F. Darchambeau, and M. Schmid. Lake Kivu: Past and Present. In J.-P. Descy, F. Darchambeau, and M. Schmid, editors, *Lake Kivu: Limnology and Biogeochemistry of a Tropical Great Lake*, pages 1–11. Springer, Dordrecht, Netherlands, 2012.

T. Dinku, S. Chidzambwa, P. Ceccato, S. J. Connor, and C. F. Ropelewski. Validation of high-resolution satellite rainfall products over complex terrain. *International Journal of Remote Sensing*, 29(14):4097–4110, 2008.

D. Docquier, W. Thiery, S. Lhermitte, and N. van Lipzig. Multi-year wind dynamics around Lake Tanganyika. *Climate Dynamics*, 47(9):3191–3202, 2016.

East African Community. Enhancing Safety of Navigation and Efficient Exploitation of Natural Resources over Lake Victoria and its Basin by Strengthening Meteorological Services on the Lake. Technical Report October, Approved by the East African Community Council of Ministers, 2011.

H. Frank and S. C. Althoen. *Statistics: concepts and applications*. Cambridge University Press, 1994.

R. James, R. Washington, B. Abiodun, G. Kay, J. Mutemi, W. Pokam, N. Hart, G. Artan, and C. Senior. Evaluating climate models with an African lens. *Bulletin of the American Meteorological Society*, 99(2):313–336, 2018.



M. W. Kimani, J. C. B. Hoedjes, and Z. Su. An assessment of satellite-derived rainfall products relative to ground observations over East Africa. *Remote Sensing*, 9(5):430, 2017.

P. A. Lange, G. v.d. Graaf, and M. Gade. Rain-induced subsurface turbulence measured using image processing methods. In *Proc. IGARSS*, volume 7, pages 3175–3177, 2000.

5 D. V. Mironov, E. Heise, E. Kourzeneva, B. Ritter, N. Schneider, and A. Terzhevik. Implementation of the lake parameterisation scheme FLake into the numerical weather prediction model COSMO. *Boreal Environment Research*, 15:218–230, 2010.

C. Morana, A. V. Borges, F. A. E. Roland, F. Darchambeau, J.-P. Descy, and S. Bouillon. Methanotrophy within the water column of a large meromictic tropical lake (Lake Kivu, East Africa). *Biogeosciences*, 12(7):2077–2088, 2015a.

10 C. Morana, F. Darchambeau, F. A. E. Roland, A. V. Borges, F. Muvundja, Z. Kelemen, P. Masilya, J.-P. Descy, and S. Bouillon. Bio-geochemistry of a large and deep tropical lake (Lake Kivu, East Africa): insights from a stable isotope study covering an annual cycle. *Biogeosciences*, 12(16):4953–4963, 2015b.

C. Morana, F. A. E. Roland, S. A. Crowe, M. Llirós, A. V. Borges, F. Darchambeau, and S. Bouillon. Chemoautotrophy and anoxygenic photosynthesis within the water column of a large meromictic tropical lake (Lake Kivu, East Africa). *Limnology and Oceanography*, 61(4):1424–1437, 2016.

15 C. M. O'Reilly, S. R. Alin, P.-D. Plisnier, A. S. Cohen, and B. a. McKee. Climate change decreases aquatic ecosystem productivity of Lake Tanganyika, Africa. *Nature*, 424(6950):766–768, 2003.

A. Prosperetti, L. A. Crum, and H. C. Pumphrey. The underwater noise of rain. *Journal of Geophysical Research: Oceans*, 94(C3):3255–3259, 1989.

C. Salles, J. Poesen, and D. Sempere-Torres. Kinetic energy of rain and its functional relationship with intensity. *Journal of Hydrology*, 257:20 256–270, 2002.

M. Schmid, M. Halbwachs, B. Wehrli, and A. Wüest. Weak mixing in Lake Kivu: New insights indicate increasing risk of uncontrolled gas eruption. *Geochemistry, Geophysics, Geosystems*, 6:Q07009, 2005.

E. D. Skillingstad and D. W. Denbo. An ocean large-eddy simulation of Langmuir circulations and convection in the surface mixed layer. *Journal of Geophysical Research: Oceans*, 100(C5):8501–8522, 1995.

25 R. Spigel and G. Coulter. Comparison of Hydrology and physical limnology of the East African Great Lakes: Tanganyika, Malawi, Victoria, Kivu and Turkana (with references to some North American Great Lakes). In T. Johnson and E. Odada, editors, *The Limnology, Climatology and Paleoclimatology of the East African lakes*, pages 103–140. Gordon and Breach Publishers, Amsterdam, The Netherlands, 1996.

M. B. Sylla, F. Giorgi, E. Coppola, and L. Mariotti. Uncertainties in daily rainfall over Africa: assessment of gridded observation products and evaluation of a regional climate model simulation. *International Journal of Climatology*, 33(7):1805–1817, 2013.

30 W. Thiery, A. Martynov, F. Darchambeau, J.-P. Descy, P.-D. Plisnier, L. Sushama, and N. P. M. van Lipzig. Understanding the performance of the FLake model over two African Great Lakes. *Geoscientific Model Development*, 7(1):317–337, 2014a.

W. Thiery, V. M. Stepanenko, X. Fang, K. D. Jöhnk, Z. Li, A. Martynov, M. Perroud, Z. M. Subin, F. Darchambeau, D. Mironov, and N. P. M. van Lipzig. LakeMIP Kivu: Evaluating the representation of a large, deep tropical lake by a set of 1-dimensional lake models. *Tellus A*, 35 66:21390, 2014b.

W. Thiery, E. L. Davin, H.-J. Panitz, M. Demuzere, S. Lhermitte, and N. P. M. van Lipzig. The Impact of the African Great Lakes on the Regional Climate. *Journal of Climate*, 28(10):4061–4085, 2015.



W. Thiery, E. L. Davin, S. I. Seneviratne, K. Bedka, S. Lhermitte, and N. P. M. van Lipzig. Hazardous thunderstorm intensification over Lake Victoria. *Nature Communications*, 7:12786, 2016.

W. Thiery, L. Gudmundsson, K. Bedka, F. H. M. Semazzi, S. Lhermitte, P. Willems, N. P. M. van Lipzig, and S. I. Seneviratne. Early warnings of hazardous thunderstorms over Lake Victoria. *Environmental Research Letters*, 12(7):074012, 2017.

5 A. A. Townsend. *The structure of turbulent shear flow*. Cambridge University Press, 1976.

L. P. H. van Beek, T. Eikelboom, M. T. H. van Vliet, and M. F. P. Bierkens. A physically based model of global freshwater surface temperature. *Water Resources Research*, 48(9), 2012. W09530.

A. van Dijk, L. Bruijnzeel, and C. Rosewell. Rainfall intensity-kinetic energy relationships: A critical literature appraisal. *Journal of Hydrology*, 261:1–23, 2002.

10 P. Verburg and J. P. Antenucci. Persistent unstable atmospheric boundary layer enhances sensible and latent heat loss in a tropical great lake: Lake tanganyika. *Journal of Geophysical Research: Atmospheres*, 115(D11), 2010. D11109.

P. Verburg and R. Hecky. The physics of the warming of Lake Tanganyika by climate change. *Limnology and Oceanography*, 54:2418–2430, 2009.

P. Verburg and R. Hecky. Wind patterns, evaporation, and related physical variables in Lake Tanganyika, East Africa. *Journal of Great Lakes Research*, 29:48–61, 2003.

15 P. Verburg, R. E. Hecky, and H. Kling. Ecological consequences of a century of warming in Lake Tanganyika. *Science*, 301(5632):505–507, 2003.

P. Verburg, J. P. Antenucci, and R. E. Hecky. Differential cooling drives large-scale convective circulation in Lake Tanganyika. *Limnology and Oceanography*, 56(3):910–926, 2011.

20 Z. Wan. New refinements and validation of the MODIS land-surface temperature/emissivity products. *Remote Sensing of Environment*, 112 (1):59–74, 2008.

N. Wei, Y. Dai, M. Zhang, L. Zhou, D. Ji, S. Zhu, and L. Wang. Impact of precipitation-induced sensible heat on the simulation of land-surface air temperature. *Journal of Advances in Modeling Earth Systems*, 6(4):1311–1320, 2014.

G. Weyhenmeyer, M. Mackay, J. Stockwell, W. Thiery, H.-P. Grossart, P. Augusto-Silva, H. Baulch, E. de Eyto, J. Hejzlar, K. Kangur, 25 G. Kirillin, D. Pierson, J. Rusak, S. Sadro, and I. Woolway. Citizen science shows systematic changes in the temperature difference between air and inland waters with global warming. *Scientific reports*, 7:43890, 2017.

B. J. Woodhams, C. E. Birch, J. H. Marsham, C. L. Bain, N. M. Roberts, and D. F. A. Boyd. What is the added value of a convection-permitting model for forecasting extreme rainfall over tropical East Africa? *Monthly Weather Review*, 146(9):2757–2780, 2018.

N. Yu, B. Boudevillain, G. Delrieu, and R. Uijlenhoet. Estimation of rain kinetic energy from radar reflectivity and/or rain rate based on a 30 scaling formulation of the raindrop size distribution. *Water Resources Research*, 48(4), 2012. W04505.

C. J. Zappa, D. T. Ho, W. R. McGillis, M. L. Banner, J. W. H. Dacey, L. F. Bliven, B. Ma, and J. Nystuen. Rain-induced turbulence and air-sea gas transfer. *Journal of Geophysical Research: Oceans*, 114(C7), 2009. C07009.



Figure 1. Map of Lake Kivu. The lower left corner of the map is at 2.6 S, 28.7 E, and the upper right corner is at 1.5 S, 29.5 E. The lake is approximately 90 km long and 50 km wide. The magenta line along the lake indicates the boundary between D.R.Congo to the west and Rwanda to the east. The weather station is situated approximately 3 km offshore, near Goma at the northern end of the lake. Its position is marked with a red square. (©OpenStreetMap contributors. Mapping data are available under the Open Database License.)



Figure 2. Automatic weather station on Lake Kivu after its installation, 8 October 2012 (©Wim Thiery). Letter **a** indicates the location of the temperature, relative humidity and radiation sensors at 4.40m above the lake surface, while **b** shows the location of the wind vane at 7.20 m above the lake surface.

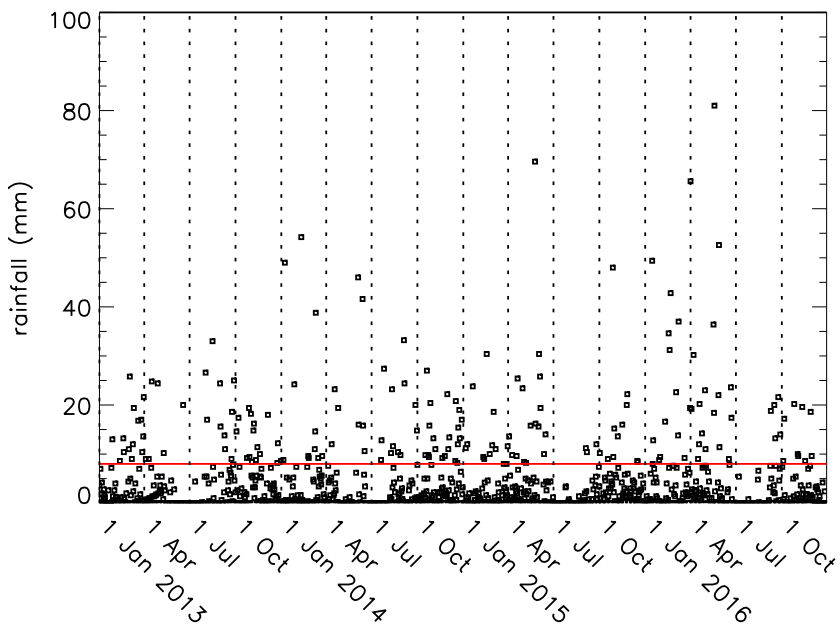


Figure 3. Daily rainfall totals for four years of the observational record, beginning on 1 January 2013. The red line marks the 8 mm point, which is used to partition rain days between WET (≤ 8 mm) and VWET(> 8 mm).

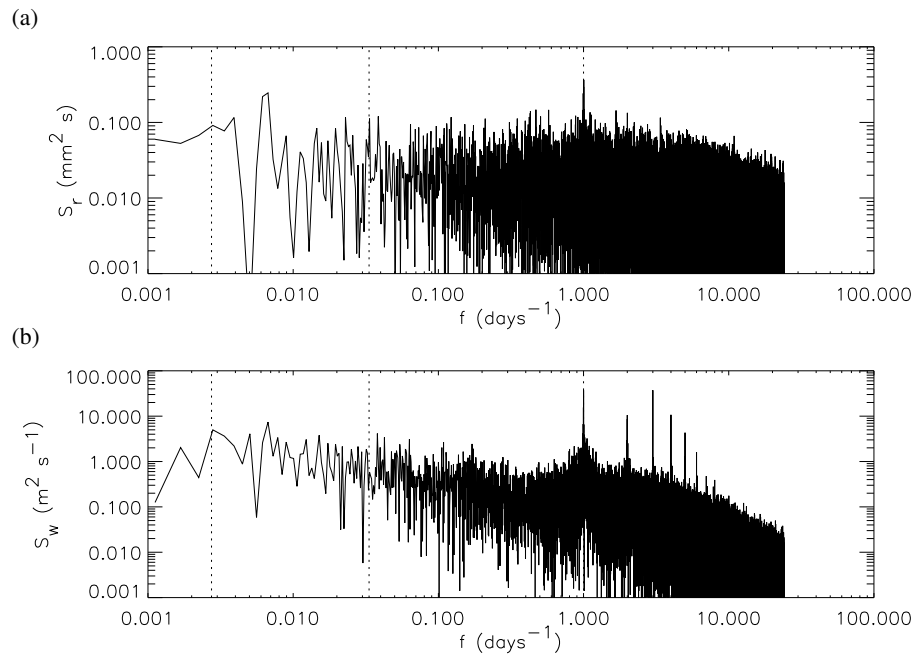


Figure 4. (a) Power spectrum of half-hourly rainfall amount (S_r , $\text{mm}^2 \text{s}$), and (b) power spectrum of half-hourly mean wind speed (S_w , $\text{m}^2 \text{s}^{-1}$), both for the period 13 September 2012 to 14 August 2017. The vertical dotted lines mark frequencies (f , days^{-1}) corresponding to 1 day, 30 days and 365 days. Both plots show a distinct peak at the daily frequency, with the wind speed also exhibiting several sub-daily peaks.

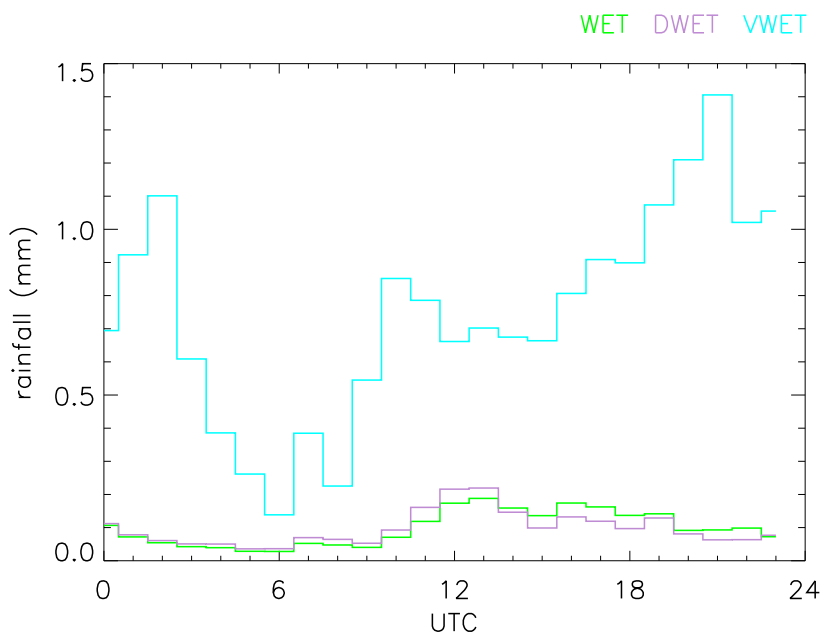


Figure 5. The average rainfall for each hour of the day, for VWET days (cyan) WET days (green) and DWET days (magenta). On this and later plots, time is shown as UTC (Universal Time Coordinate), which is 2 hours behind LT (Local Time) i.e. LT = UTC + 2 h.

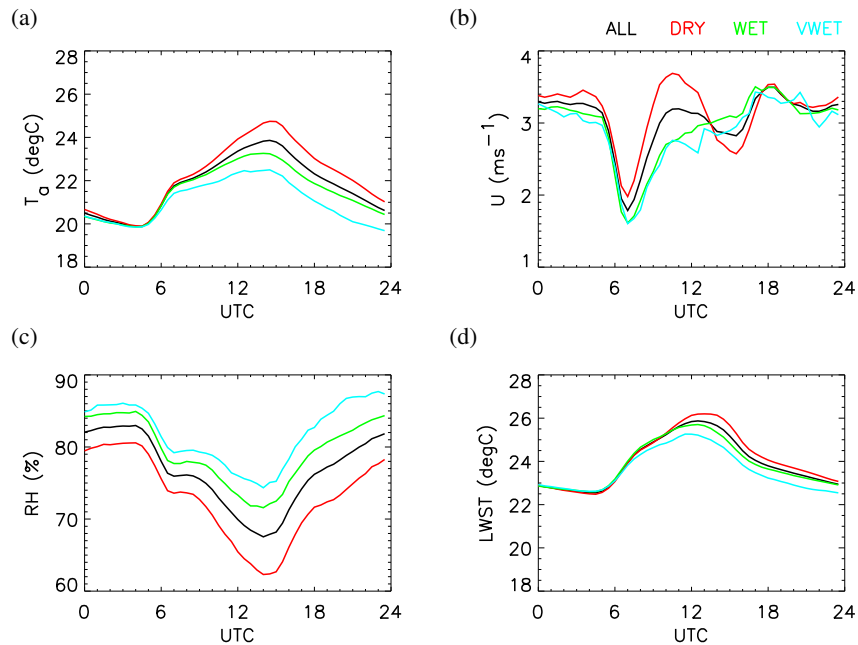


Figure 6. Mean diurnal cycles of (a) air temperature (T_a , $^{\circ}\text{C}$), (b) wind speed (U , m s^{-1}), (c) relative humidity (RH, %), (d) lake surface temperature (LWST, $^{\circ}\text{C}$) from the upwelling longwave irradiance, assuming an emissivity of 0.99. The input data are those from the four years 2013-2016 of the campaign, to represent all seasons equally. The colours correspond to diurnal cycles averaged over ALL days (black), DRY days (red), WET days (green) and VWET days (cyan).

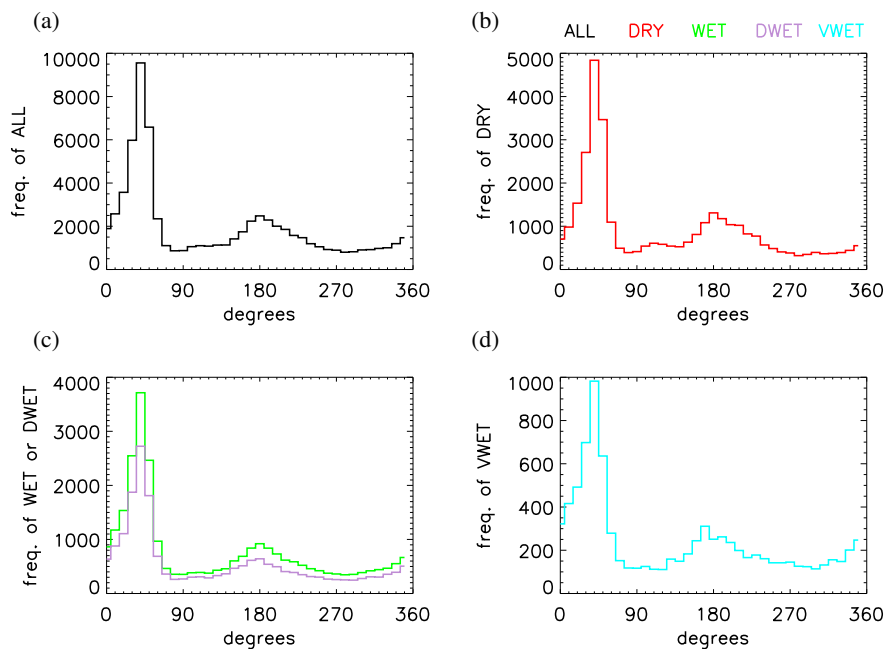


Figure 7. Histograms of half-hourly mean wind direction for 2013–2016. The colours are the same as in figures 5 and 6.

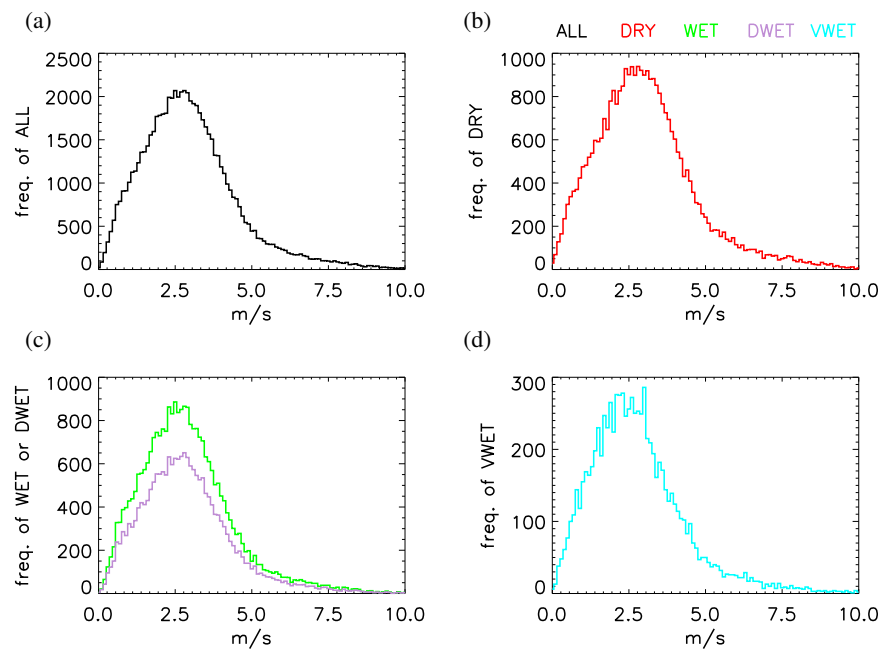


Figure 8. Histograms of half-hourly mean wind speed for 2013–2016. The colours are the same as in figures 5 and 6.

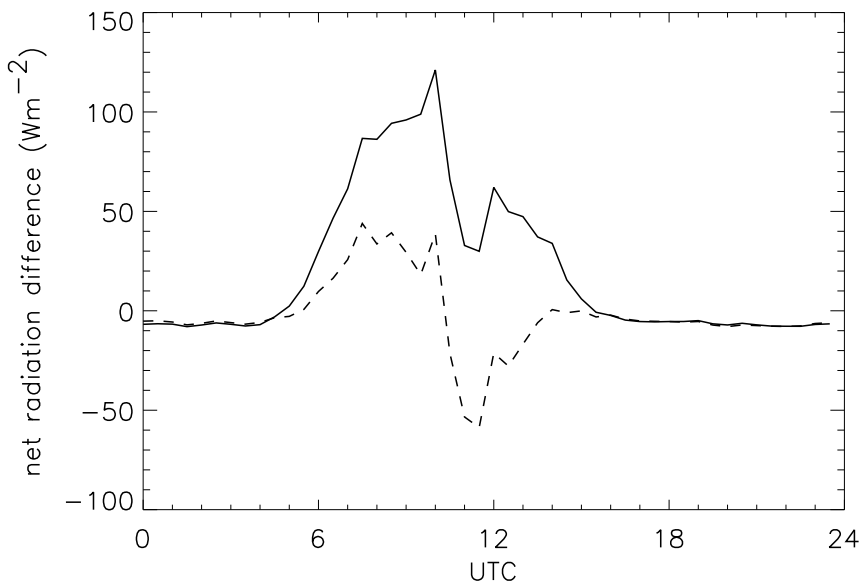


Figure 9. Comparison of the differences in net radiation. WET minus VWET net radiation is the solid line, and DWET minus VWET net radiation is the dashed line.

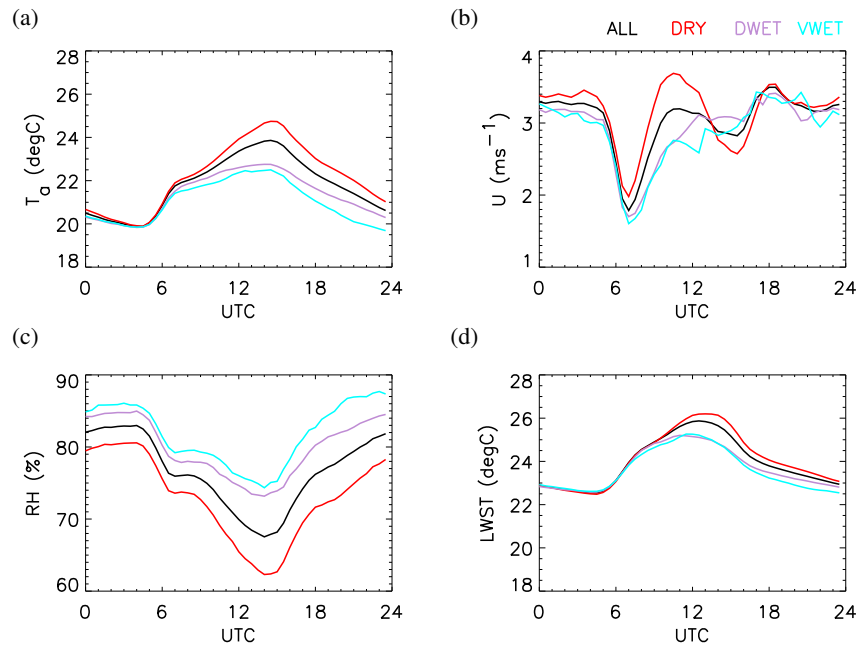


Figure 10. Mean diurnal cycles of (a) air temperature (T_a , $^{\circ}\text{C}$), (b) wind speed (U , m s^{-1}), (c) relative humidity (RH, %), (d) lake surface temperature (LWST, $^{\circ}\text{C}$) from the upwelling longwave irradiance, assuming an emissivity of 0.99. The input data are those from the four years 2013-2016 of the campaign, to represent all seasons equally. The colours correspond to diurnal cycles averaged over ALL days (black), DRY days (red), DWET days (magenta) and VWET days (cyan).

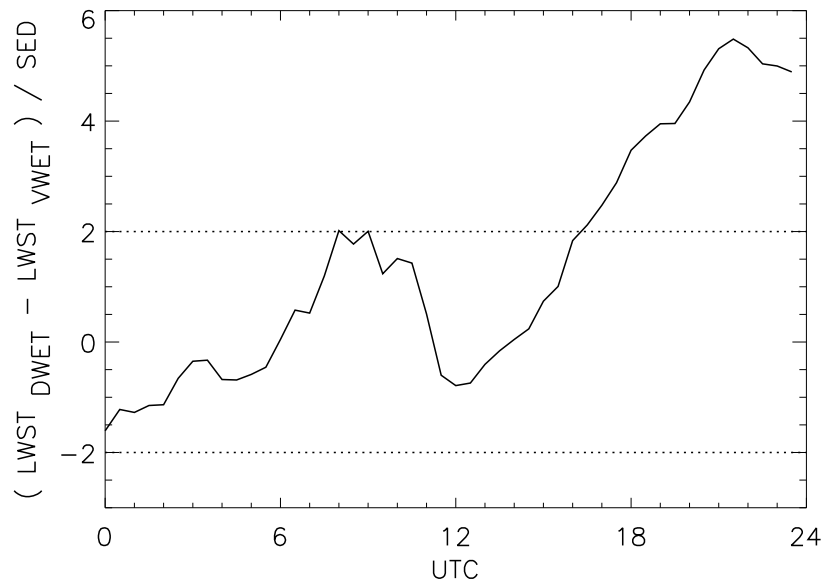


Figure 11. Diurnal behaviour of the difference in mean values of LWST in the DWET and VWET cases, normalised by the standard error of the difference, SED , see (2). The dotted lines show ± 2 standard deviations for this statistic. It may be seen that the value climbs above 2 at later times, indicating the significance of the difference in the means then.